

## THE INFRARED MORPHOLOGY OF GALACTIC CENTERS

C. M. Telesco, R. Decher, and B. D. Ramsey  
Space Science Laboratory, NASA Marshall Space Flight Center

R. D. Wolstencroft and S. G. Leggett  
Royal Observatory, Edinburgh

ABSTRACT. We present initial results of a program to map the centers of galaxies in the mid-infrared using the NASA-MSFC 20-pixel bolometer array. Maps at  $10.8 \mu\text{m}$  of the galaxies NGC 5236 (M83), NGC 1808, NGC 4536, and NGC 4527 reveal complex emitting regions ranging in size from 500 pc to 2 kpc. The infrared spatial distributions generally resemble those in the visible and radio. In all cases a large fraction of the IRAS  $12 \mu\text{m}$  flux originates in spatial structures prominent in the maps.

## 1. INTRODUCTION

The central regions of many galaxies emit intense radiation at  $\lambda > 5 \mu\text{m}$  usually attributed to warm dust. Complexes of young stars and, in some cases, non-thermal sources appear to play a key role in heating the dust, but our understanding of this phenomenon is severely limited by our not knowing how the emission is spatially distributed in the centers of a large sample of galaxies. We must be able to relate their infrared spatial structure to fundamental galactic properties determined throughout the spectrum.

Although numerous galaxies have been observed at  $\lambda > 10 \mu\text{m}$  by IRAS and from the ground, these survey data are either of low spatial resolution, as in the case of IRAS, or obtained with a single small focal-plane aperture (typically 6" in diameter) centered on a visually prominent position. Multi-aperture observations (e.g., Rieke 1976) have established scale sizes for central infrared-emitting regions in a few galaxies, while mapping (e.g., Telesco and Gatley 1984) has defined the details of the infrared spatial distributions in several others. However, single-beam infrared mapping is very time consuming, and the list of mapped galaxies is still short; only nine were mapped prior to the present study. To address this problem, we at NASA Marshall Space Flight Center have developed a 20-pixel bolometer spatial array for use at 10-30  $\mu\text{m}$ . This array has substantially increased our mapping speed, as illustrated by the fact that the total time required to map the four galaxies discussed here was less than half an observing night.

## 2. OBSERVATIONS AND ANALYSIS

The maps were made at  $10.8 \mu\text{m}$  ( $\Delta\lambda = 5.3 \mu\text{m}$ ) and were obtained at the NASA Infrared Telescope Facility in 1985 November (NGC 1808) and 1986 March (M83, NGC 4536, and NGC 4527). The 20 array pixels were arranged in a 5 x 4 (RA x Dec) configuration with each square pixel having dimensions (FWHM)  $4".3 \times 4".3$ . The pixel center-to-center separation was  $4".5$ . All maps are presented here at the same scale, with the pixel size shown in Figure 2. Except for the lower 5" of

the map of NGC 1808, the separation between adjacent observed positions was one-half pixel. The lowest contours drawn in each map correspond to a signal-to-noise ratio  $\geq 2$ , and the mapped regions are enclosed by dashed lines. In these maps, the cross designates the visually prominent position used for guiding at the telescope. We have also found that the  $2 \mu\text{m}$  peaks, which correspond to the true nuclei as defined by the peaks in the mass distribution of old stars, are coincident with the visible nuclei in M83, NGC 4536, and NGC 4527.

The four galaxies are bright IRAS far-infrared sources also detected by IRAS at 12 and  $25 \mu\text{m}$ . The quoted flux densities are for  $10.8 \mu\text{m}$ , but before comparison of our and IRAS fluxes, our flux densities are converted to equivalent  $12 \mu\text{m}$  values using the 12 and  $25 \mu\text{m}$  spectral slope, which is also used to color-correct the  $12 \mu\text{m}$  IRAS data. Presented flux uncertainties do not include the  $\pm 10\%$  inherent in the absolute flux calibration.

### 3. RESULTS

Our  $10.8 \mu\text{m}$  maps are fully reduced, but our analysis of these data is in progress. These results are therefore presented without significant interpretation. Preliminary comparison of the central infrared sources with available radio and visual images shows that the shapes are similar. The study of detailed correspondance (or lack thereof) of structure at various wavelengths must await the accurate relative positioning of our maps with respect to radio and visual images, a procedure now underway. Note that quoted infrared luminosities correspond to the range  $10\text{--}300 \mu\text{m}$  and have been estimated by assuming a reasonable extrapolation beyond  $100 \mu\text{m}$  (see Telesco and Harper 1980). We have also assumed that the energy distribution at each position in a map resembles that observed from the whole region.

#### 3.1 NGC 5236 (M83)

The total  $10.8 \mu\text{m}$  flux density in our map of NGC 5236 (Figure 1) is  $3.3 \pm 0.2 \text{ Jy}$ , which accounts for 80% of the IRAS  $12 \mu\text{m}$  flux. The diameter of the lowest contour is  $500 \text{ pc}$  at  $6 \text{ Mpc}$ , and the total source luminosity is  $\sim 1 \times 10^{10} L_{\odot}$ . Each of the two  $10.8 \mu\text{m}$  peaks emits  $\sim 1 \times 10^9 L_{\odot}$  in a region  $130 \text{ pc}$  in size. It is noteworthy that no prominent infrared source occurs at the visual and  $2 \mu\text{m}$  nucleus. The infrared map bears a striking resemblance to the  $21 \text{ cm}$  map presented by Condon et al. (1982). The visual properties of the region spanned by our map are dominated by normal

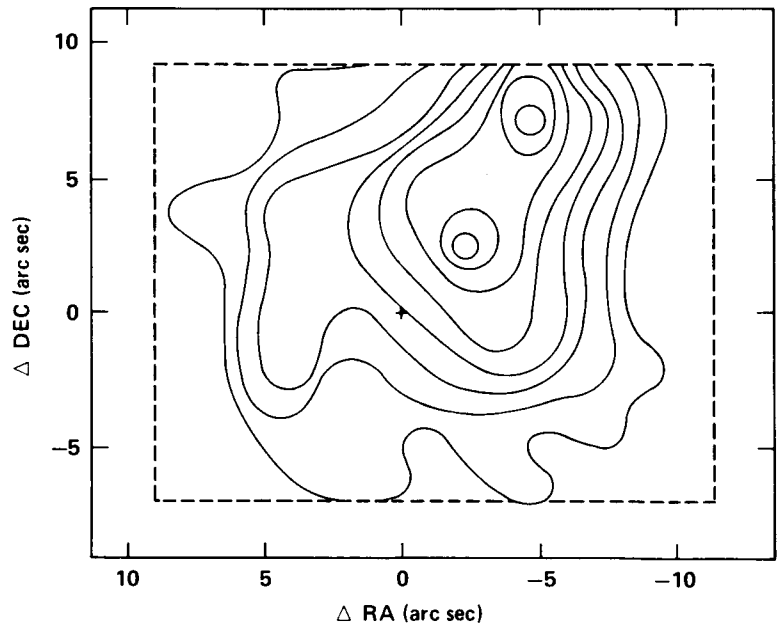


Figure 1. NGC 5236 (SBc) at  $10.8 \mu\text{m}$ . The contour levels (mJy/pixel) are: 100, 150, 200, 250, 300, 350, 400, and 450.

HII regions (Pastoriza 1975), which, along with the infrared energy distribution, implies that the complicated and extended infrared emission is powered by young stars. A dust lane in the galactic bar enters the field near the bright infrared sources to the northwest. Another dust lane enters the field near the tongue-like feature in the southeast. We speculate that gas flow along the bar may be feeding the star formation which is occurring at rates (OBA stars) of  $3 M_{\odot} \text{ yr}^{-1}$  throughout the mapped region and  $0.4 M_{\odot} \text{ yr}^{-1}$  at the peaks.

### 3.2 NGC 1808

The  $10.8 \mu\text{m}$  flux density within the lowest contour of our map of NGC 1808 (Figure 2) is  $2.5 \pm 0.1 \text{ Jy}$ , which accounts for 69% of the flux in the IRAS  $12 \mu\text{m}$  band. The remaining IRAS flux can be accounted for by lower level emission in the mapped region. The luminosity within the lowest contour, which has a maximum dimension of 1 kpc at 11 Mpc, is  $2 \times 10^{10} L_{\odot}$ . The peak luminosity is  $5 \times 10^9 L_{\odot}$  from a region 230 pc in size. NGC 1808 appears to contain a weak Seyfert nucleus embedded in a bright emission-line region ionized by young stars (Véron-Cetty and Véron 1985). Our map implies that the Seyfert nucleus emits  $< 25\%$  of the infrared luminosity. The most intense IR emission originates in a region  $200 \text{ pc} \times 400 \text{ pc}$  in size which, if the lower visual and infrared contours coincide, is centered on the Seyfert nucleus.

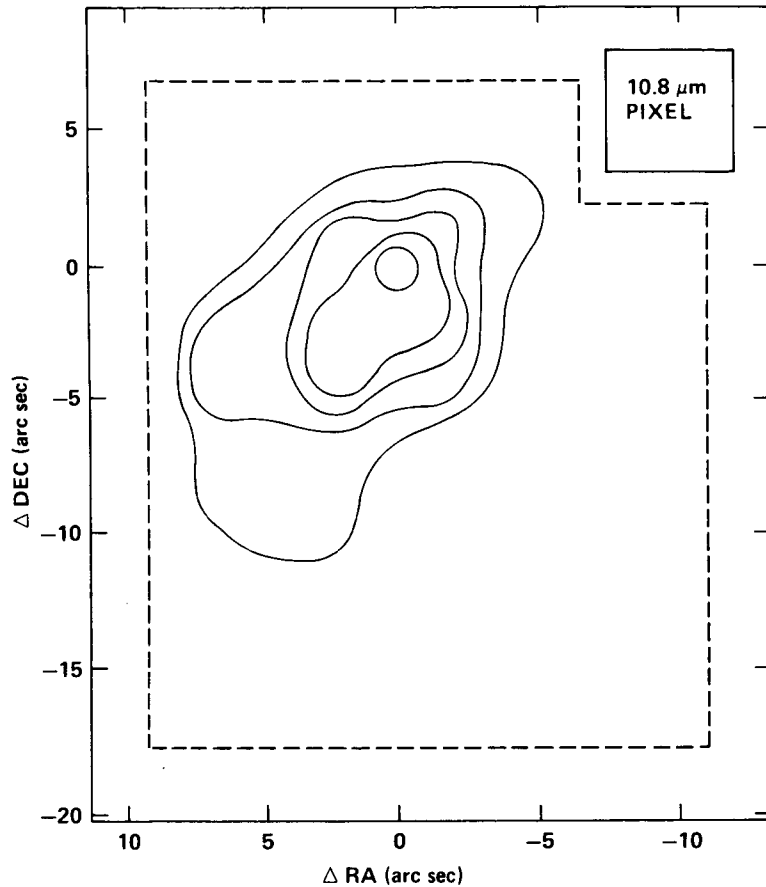


Figure 2. NGC 1808 (Sbc pec.) at  $10.8 \mu\text{m}$ . The contour levels (mJy/pixel) are: 200, 300, 400, 500, and 600.

### 3.3 NGC 4536 and NGC 4527

The  $10.8 \mu\text{m}$  flux density within the lowest contour of our map of NGC 4536 (Figure 3) is  $0.43 \pm 0.03 \text{ Jy}$ . From the entire mapped region, we detect  $0.70 \pm 0.09 \text{ Jy}$ , which accounts for 57% of the IRAS  $12 \mu\text{m}$  flux. The total infrared luminosity within the lowest contour, which has a long dimension of 1.4 kpc at 22 Mpc, is  $1.4 \times 10^{10} L_{\odot}$ . The peak luminosity is  $5 \times 10^9 L_{\odot}$  from a region 460 pc in size and originates within  $1''$  of the visual peak. The shape of the infrared source in NGC 4536 closely resembles that of the radio continuum emission (Condon et al. 1982).

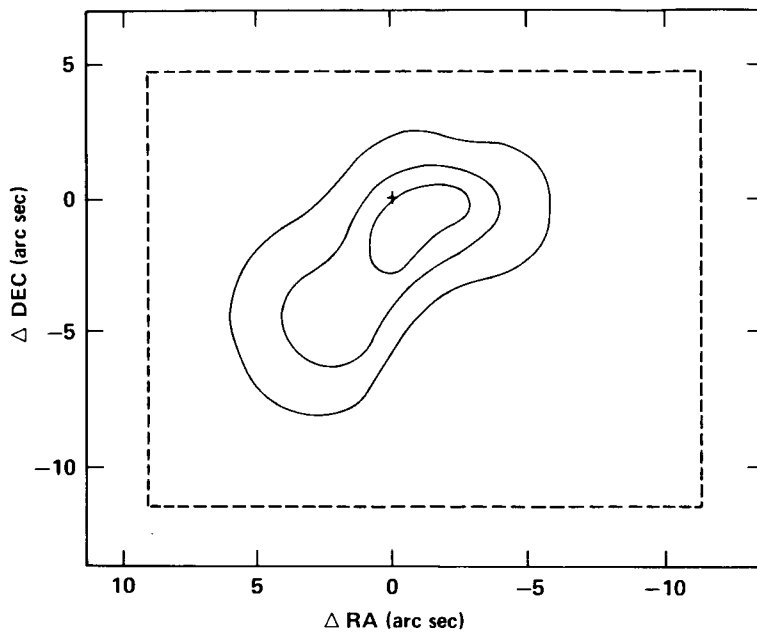
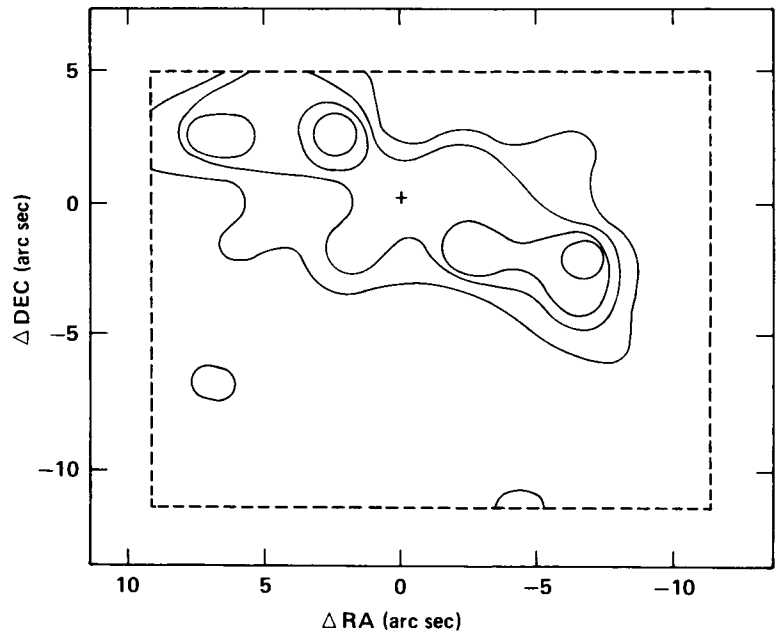


Figure 3. NGC 4536 (Sc) at  $10.8 \mu\text{m}$ . The contour levels (mJy/pixel) are: 50, 100, and 150.

The  $10.8 \mu\text{m}$  flux density from NGC 4527 (Figure 4) is  $0.51 \pm 0.04 \text{ Jy}$  within the lowest contour, which accounts for 54% of the IRAS  $12 \mu\text{m}$  flux. The lowest infrared contour has a long dimension of 2 kpc at 21 Mpc. The luminosity within the lowest contour is  $3 \times 10^{10} L_{\odot}$ , with  $7 \times 10^9 L_{\odot}$  originating in a 430 pc region centered on each of the two brightest peaks. Although the complicated emission region is roughly centered on the visual peak, no obvious infrared peak occurs there.

Figure 4. NGC 4527 (Sb) at  $10.8 \mu\text{m}$ . Contour levels (mJy/pixel) are: 50, 75, 100, and 125.



#### REFERENCES

- Condon, J. J., Condon, M. A., Gisler, G., and Puschell, J. J. 1982, *Ap. J.*, 252, 102.
- Pastoriza, M. G. 1975, *Astrophys. Sp. Sci.*, 33, 173.
- Rieke, G. H., 1976, *Ap. J. (Letters)*, 206, L15.
- Telesco, C. M., and Gatley, I. 1984, *Ap. J.*, 284, 557.
- Telesco, C. M., and Harper, D. A. 1980, *Ap. J.*, 235, 392.
- Véron-Cetty, M.-P., and Véron, P. 1985, *Astron. Astrophys.*, 145, 425.